



Label-free super-resolution imaging below 90-nm using photon-reassignment

Alberto Aguilar, Adeline Boyreau, Pierre Bon

► To cite this version:

Alberto Aguilar, Adeline Boyreau, Pierre Bon. Label-free super-resolution imaging below 90-nm using photon-reassignment. 2021. hal-03405548

HAL Id: hal-03405548

<https://hal.science/hal-03405548>

Preprint submitted on 5 Nov 2021


HAL is a multi-disciplinary open access archive for the deposit and dissemination of scientific research documents, whether they are published or not. The documents may come from teaching and research institutions in France or abroad, or from public or private research centers.

L'archive ouverte pluridisciplinaire **HAL**, est destinée au dépôt et à la diffusion de documents scientifiques de niveau recherche, publiés ou non, émanant des établissements d'enseignement et de recherche français ou étrangers, des laboratoires publics ou privés.



RESEARCH ARTICLE

Label-free super-resolution imaging below 90-nm using photon-reassignment [version 1; peer review: awaiting peer review]

Alberto Aguilar^{1,2}, Adeline Boyreau^{1,2}, Pierre Bon^{1,2} 

¹Laboratoire Photonique Numérique et Nanosciences (LP2N), UMR 5298, Université Bordeaux, Talence, 33400, France

²LP2N UMR 5298, CNRS & Institut d'Optique, Talence, 33400, France

v1 First published: 24 Mar 2021, 1:3
<https://doi.org/10.12688/openreseurope.13066.1>
Latest published: 24 Mar 2021, 1:3
<https://doi.org/10.12688/openreseurope.13066.1>

Open Peer Review

Reviewer Status Awaiting Peer Review

Any reports and responses or comments on the article can be found at the end of the article.

Abstract

Background: Achieving resolutions below 100 nm is key for many fields, including biology and nanomaterial characterization. Although nearfield and electron microscopy are the gold standards for studying the nanoscale, optical microscopy has seen its resolution drastically improve in the last decades. So-called super-resolution microscopy is generally based on fluorescence photophysics and requires modification of the sample at least by adding fluorescent tags, an inevitably invasive step. Therefore, it remains very challenging and rewarding to achieve optical resolutions beyond the diffraction limit in label-free samples.

Methods: Here, we present a breakthrough to unlock label-free 3D super-resolution imaging of any object including living biological samples. It is based on optical photon-reassignment in confocal reflectance imaging mode.

Results: We demonstrate that we surpass the resolution of all fluorescence-based confocal systems by a factor ~ 1.5 . We have obtained images with a 3D (x,y,z) optical resolution of (86x86x248) nm³ using a visible wavelength (445 nm) and a regular microscope objective (NA=1.3). The results are presented on nanoparticles as well as on (living) biological samples.

Conclusions: This cost-effective approach double the resolution of reflectance confocal microscope with minimal modifications. It is therefore compatible with any microscope and sample, works in real-time, and does not require any signal processing.

Keywords

Super-resolution imaging, Label-free imaging, confocal reflectance microscopy



This article is included in the [Excellent Science](#) gateway.

Corresponding author: Pierre Bon (pierre.bon@cnrs.fr)

Author roles: **Aguilar A:** Data Curation, Formal Analysis, Methodology, Resources, Software, Visualization, Writing – Original Draft Preparation, Writing – Review & Editing; **Boyreau A:** Resources; **Bon P:** Conceptualization, Formal Analysis, Funding Acquisition, Investigation, Project Administration, Software, Supervision, Validation, Visualization, Writing – Original Draft Preparation, Writing – Review & Editing

Competing interests: No competing interests were disclosed.

Grant information: This research was financially supported by the European Union's Horizon 2020 research and innovation programme under the grant agreement No 848645 (project SPECIPHIC). This work was also supported by CNRS and IdEx Bordeaux (ANR-10-IDEX-03-02).

The funders had no role in study design, data collection and analysis, decision to publish, or preparation of the manuscript.

Copyright: © 2021 Aguilar A *et al.* This is an open access article distributed under the terms of the [Creative Commons Attribution License](#), which permits unrestricted use, distribution, and reproduction in any medium, provided the original work is properly cited.

How to cite this article: Aguilar A, Boyreau A and Bon P. **Label-free super-resolution imaging below 90-nm using photon-reassignment [version 1; peer review: awaiting peer review]** Open Research Europe 2021, 1:3 <https://doi.org/10.12688/openreseurope.13066.1>

First published: 24 Mar 2021, 1:3 <https://doi.org/10.12688/openreseurope.13066.1>

Plain language summary

The resolution of an imaging system is a key parameter since it allows observation of smaller details and thus increases the knowledge about the observed sample. Although essential for studying living samples, optical microscopy has intrinsic resolution barriers which preclude the observation of details smaller than a few 100's of nanometer without modifying the samples (e.g. by adding fluorescent tags). However, reaching the nanoscale on unmodified objects without damaging them is essential to understand the intimate structure of the matter. Here we propose a method based on point scanning (confocal) microscopy that allows resolution below 90 nm on any samples and we demonstrate our imaging capability on living cells and nanomaterials.

Introduction

Achieving resolutions below 100 nm is key for many fields, including biology and nanomaterial characterization. Although nearfield and electron microscopy are the gold standards for studying the nanoscale, optical microscopy has seen its resolution drastically improve in the last decades¹⁻⁶. So-called super-resolution microscopy is generally based on fluorescence photophysics⁷ and requires modification of the sample at least by adding fluorescent tags, an inevitably invasive step. Optical imaging systems based on confocal microscopy (CM) grant both efficient 3D resolution and optical sectioning ability, and are thus widely spread. The majority of CMs are dedicated to image fluorescent-labeled samples, providing images with molecular specificity. The last three decades of improvement are therefore chiefly linked to the enhancement of fluorescence imaging⁸⁻¹⁰. However, fluorescent tags are dim and fragile, which limits both the acquisition rate and the duration of studies. Labeling is moreover invasive by nature, and it remains very challenging and practically impossible to label samples while ensuring reliable innocuousness (e.g. human grafts or embryos). Label-free imaging is thus key for many applications, including medical diagnostics, and is generally based on recording the light back-scattered by the sample. In this scope, optical coherence tomography¹¹⁻¹³ - including its confocal scheme¹⁴ - and reflectance confocal microscopy (RCM)¹⁵ are the most used techniques. RCM has been demonstrated to be efficient for various biomedical applications including skin imaging¹⁶⁻¹⁸, ophthalmology^{19,20}, and neuro-biology^{21,22}. However, label-free microscopy remains limited in term of resolution as compared to fluorescence-based systems.

One elegant and efficient way to increase the resolution of CM-based setups consists not only of counting the number of photons passing through the confocal detection pinhole with a mono-detector (e.g. avalanche) photodiode) but effectively recording the spatial distribution of the light transmitted by the pinhole using a 2D sensor (e.g. CCD or CMOS camera). This 2D signal is then (digitally or optically) shrunk before shifting to the next scan point in the sample. Optical super-resolution is obtained since the collected point spread function (PSF) is re-allocated into a distance where the spatial information of the adjacent PSFs can be optically resolved. The concept

of photon reassignment has been originally described by Sheppard²³ and has been implemented in fluorescence CM²⁴⁻²⁶ (resolution gain of about $\times 1.5$), Raman microscopy²⁷ (resolution gain up to $\times 1.41$), and two-photon microscopy^{28,29} (resolution gain $\times 1.81$). However, by applying this concept to RCM, it is possible to obtain a true doubling of the lateral resolution since there is no Stokes-shift between the excitation and detection wavelengths. DuBose *et al.* recently demonstrated the first example of photon reassignment for resolution enhancement in reflectance ophthalmology³⁰ (i.e. with micrometer resolution, the eye being the last focusing optics).

We present in this article a method to enhance CM resolution by using a fully-optical photon reassignment method and a reflectance-based imaging scheme. This approach grants: (i) instant super-resolution imaging even at depth ($> 100 \mu\text{m}$) without any computation; (ii) a lateral resolution below 90 nm, an axial resolution below 250 nm using visible light; and (iii) compatibility with any sample including nanomaterials and living label-free biological samples.

Results

We have designed an approach with a penetration depth of hundreds of micrometers, low photo-induced damage (i.e. no-UV light, average light power over the field of view $< 100 \text{ W/cm}^2$ for a signal to noise ratio > 100), a temporal resolution below 1 second, and a spatial resolution better than 90 nm. To do so, we use a 445 nm light source and a high numerical aperture microscope objective compatible with thick sample imaging (Silicon immersion 60x, NA=1.3, WD=0.3mm) (see [Figure 1a](#), Methods and associated [Figure 5](#) for a complete description of the optical setup). The laser is focused on the sample with a diffraction-limited size and laterally scanned with a 2D-mirror. The back-scattered light is then filtered by a confocal pinhole. The image of the confocal pinhole is re-scanned directly onto a 2D camera sensor with a doubled scanning-amplitude as compared to the object plane. This induces a two-fold reduction of the effective PSF in the image plane. The diffraction-limited PSF of diameter d is collected from the sample with a separation distance of s , as illustrated in [Figure 1a](#).

The collected PSF is rescanned into the 2D detector, maintaining the same diameter d but with a separation distance of $2s$. This fully-optical photon-reassignment directly leads to super-resolved images without requiring any computation (see *Extended data: Annex 1* for theoretical explanations³¹). We named this approach rescanned-RCM as compared to regular-RCM, where the image is reconstructed point-by-point in a de-scanned mode. As an example, in [Figure 1b-f](#) the resolving capabilities of rescanned-RCM is largely improved as compared to regular-RCM when imaging nanoparticles (100-nm gold nanobeads). In [Figure 2](#), an example of resolution enhancement on high-resolution US Air Force resolution target is also presented.

To quantify the performance of our setup, we focus on (i) the lateral and axial resolution enhancement, we then discuss

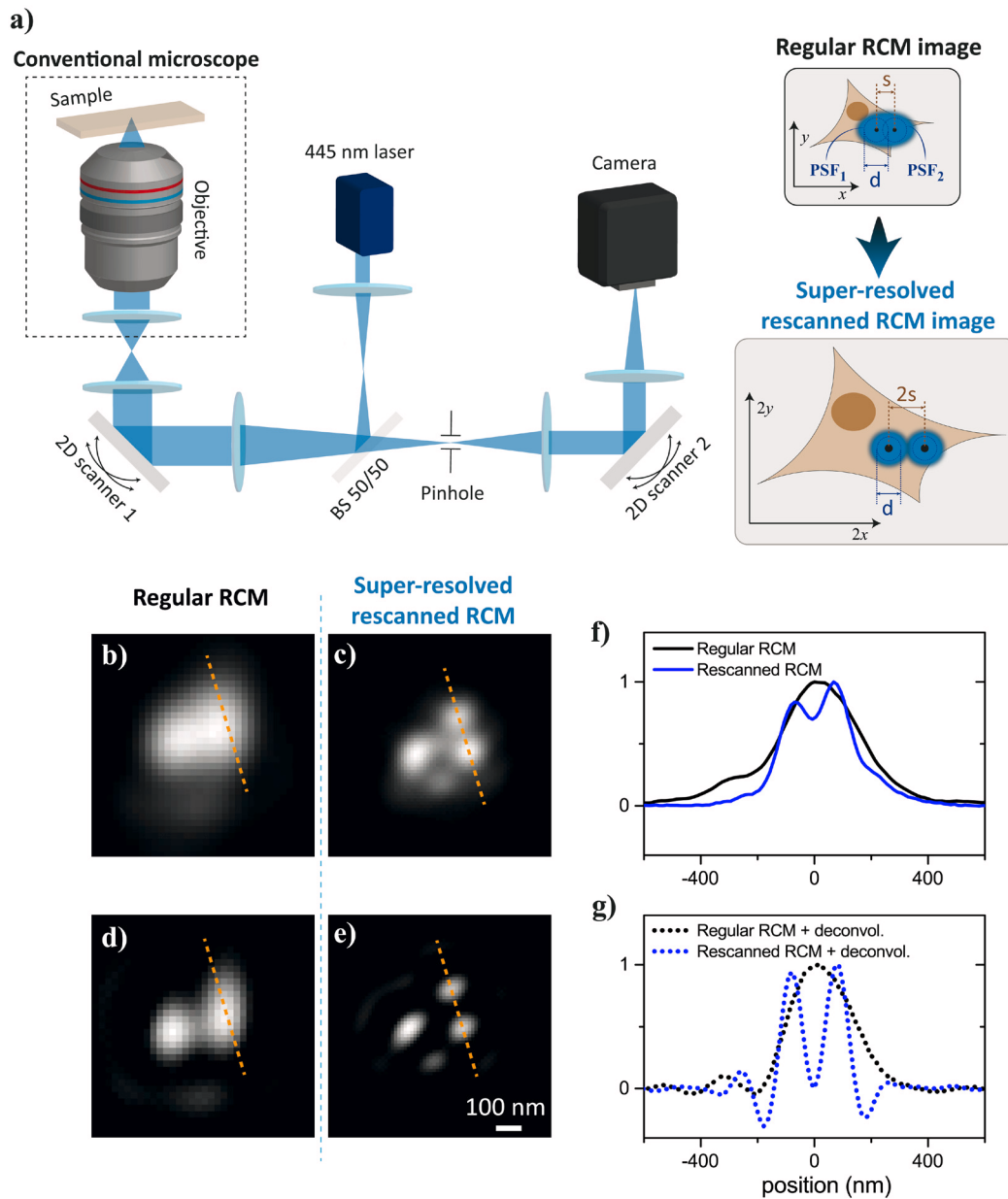


Figure 1. (a) Experimental setup and concept to achieve label-free confocal super-resolution, BS 50/50 is a 50%;50% non-polarizing beamsplitter (see Methods for detailed information). (b) 100 nm gold beads observed with conventional reflectance confocal microscopy (RCM). (c) Same zone as for (b) observed with rescanned-RCM. (d) Deconvolution of (b). (e) Deconvolution of (c). (f) Line-out of (b,c). (g) Line-out of (d,e).

(ii) the background rejection capability and (iii) present 3D biological sample reconstructions on quasi-metrological samples (diatom shells in water), and living adherent cells with a focus on intra-cellular organelle dynamics.

Resolution enhancement

Here we compare the lateral and axial 3D PSF and the associated 2D and 3D modulation transfer function (MTF) of both

regular-RCM and rescanned-RCM on 60 nm gold nanoparticles (see Methods) acting as point-objects. For a fair comparison between an optimal conventional RCM (recorded on a monodetector) and the super-resolved rescanned-RCM, the optical setup has been upgraded to have both RCM modalities running in parallel for simultaneous acquisition (see Methods for the detailed dual-modality setup). Qualitatively first, the PSF size in the rescanned mode is reduced in comparison with

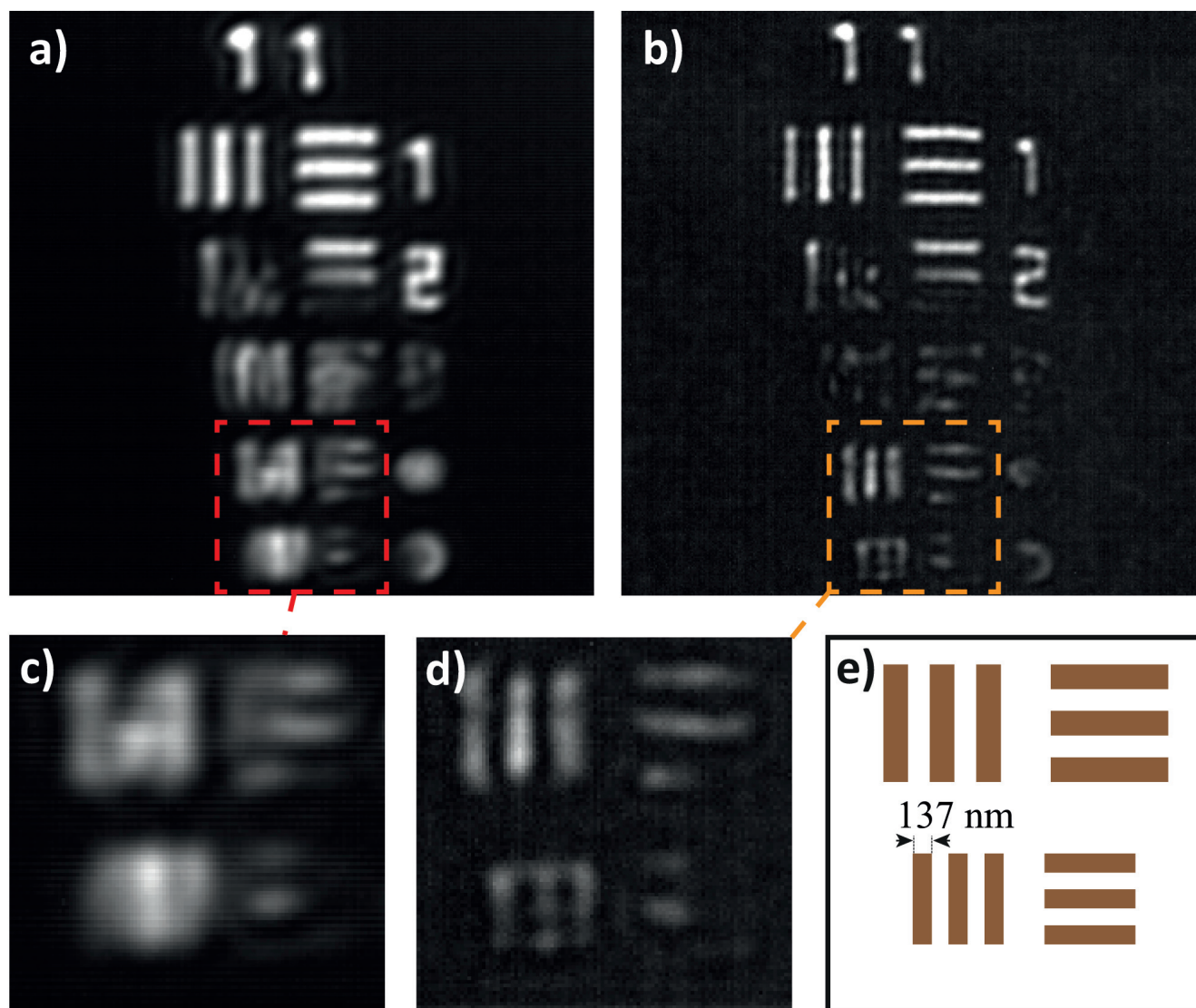


Figure 2. High-resolution positive US Air Force target element 11 observed by (a) regular reflectance confocal microscopy (RCM); (b) re-scanned RCM; (c,d) zoom in of the elements 11-4 and 11-5 from the target in (a) and (b), respectively; and (e) scheme of the theoretical resolution target. Images are 2D deconvolved.

the standard PSF of a regular-RCM (Figure 3a–d). The gain is even clearer when looking at the Fourier domain: the frequency support of the rescanned-RCM image is extended as compared to the frequency support of the regular-RCM image (Figure 3e and 3f).

To quantitatively determine the actual resolution of the microscope and its imaging performance, we have computed the 2D MTFs from both re-scanned and regular RCM frequency supports (Figure 3g). The lateral resolutions of the microscopes have been measured to be $r_{xy}^{RCM} = 171 \pm 5$ nm for the regular RCM and $r_{xy}^{srRCM} = 86 \pm 3$ nm for the re-scanned

RCM (consistent with the theoretical resolution value

$$r_{xy}^{th,srRCM} = \frac{\lambda}{4NA} = 86 \pm 5 \text{ nm}).$$

A twofold lateral resolution enhancement as compared to the regular RCM can thus be achieved using the setup in Figure 1.

Although the effect on the axial resolution of re-scanning has been investigated for fluorescence CM (and even enhanced using structured illumination³²), we didn't find any demonstration of the effect on the axial resolution for the reflectance-imaging scheme. Figure 3b and 3d demonstrate that rescanning the pinhole-image on a 2D sensor not only increases the lateral resolution but also the axial one. The

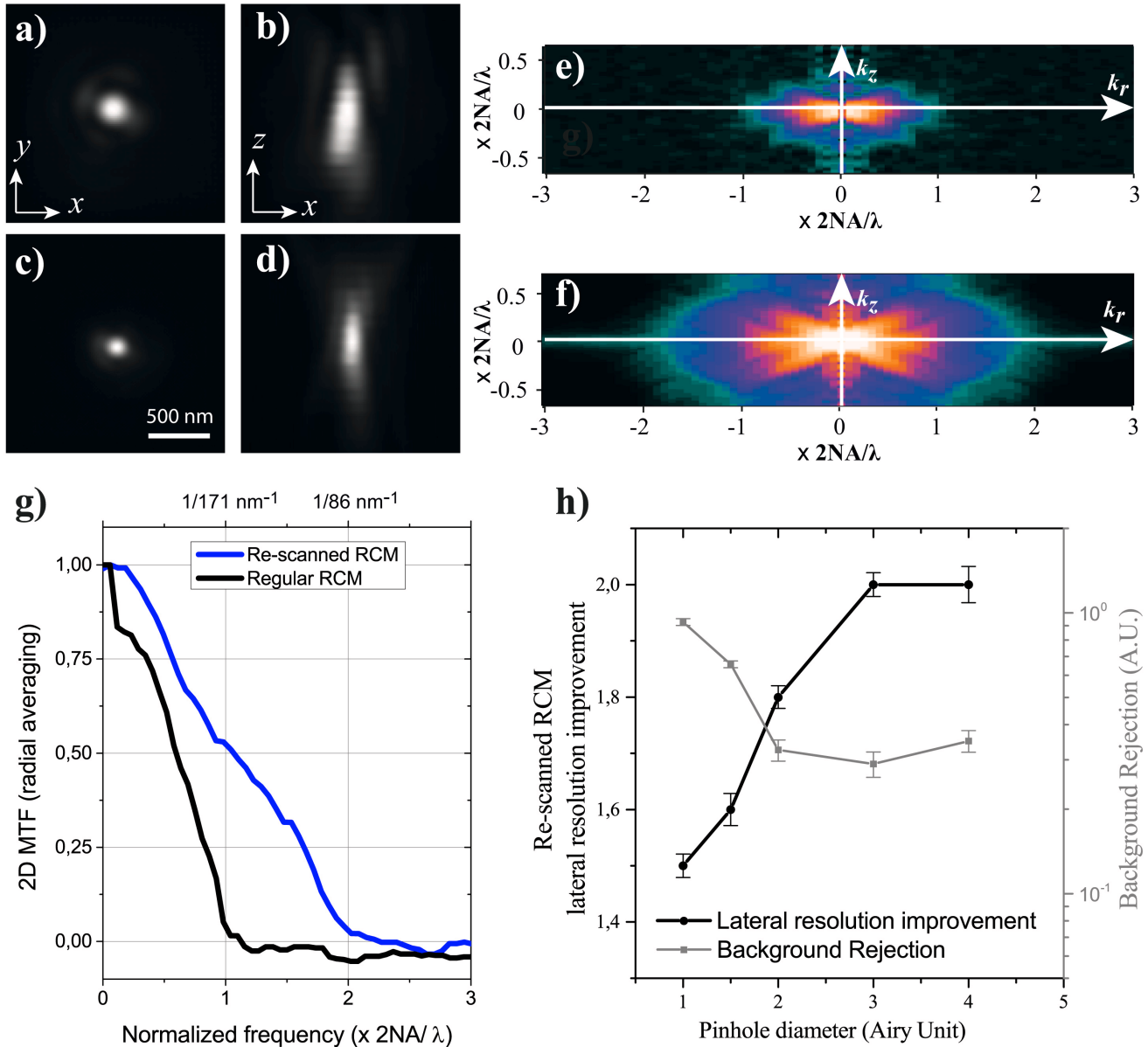


Figure 3. Experimental results of the point spread function (PSF), modulation transfer function (MTF), and background rejection of regular (pinhole of 1 Airy-size) and re-scanned super-resolved reflectance confocal microscopy (RCM), measured on 60 nm gold beads embedded in immersion oil. (a) (x, y) PSF of regular RCM; (b) (x, z) PSF of regular RCM; (c) (x, y) PSF of re-scanned-RCM; (d) (x, z) PSF of re-scanned-RCM; (e) numerical 3D Fourier transform of regular RCM PSF (radial average of each k_z plane); (f) numerical 3D Fourier transform of re-scanned RCM PSF (radial average of each k_z plane); (g) 2D MTF of regular and re-scanned RCM obtained by radial average of (a) and (c), respectively; (h) experimental results on the relation between the re-scan pinhole size and both lateral resolution and background rejection in the microscope. Resolution and background rejection normalized by those measured with regular RCM (pinhole size of 1 Airy Unit).

frequency support (Figure 3e and 3f) is also increased along the axial direction k_z when using re-scanned RCM. We experimentally determined the axial resolution of the re-scanned RCM to be $r_z^{srRCM} = 248 \pm 8 \text{ nm}$

as compared to the regular RCM theoretical axial resolution of $r_z^{th,RCM} \approx \frac{1.4\lambda}{NA^2} = 373 \text{ nm}$. This gain of 1.5 ± 0.05 is consistent with the experimental gain measured at 1.4 ± 0.1 .

Relation between background rejection and resolution

Another important aim of confocality lies in its out-of-focus light rejection capability. This aptitude is linked to the pinhole diameter with respect to the PSF size (the so-called

$$\text{AiryUnit} = \frac{1.22\lambda}{NA}$$

). Both background rejection value (using a Sandison *et al.* approach³³) and lateral resolution have been computed, varying the pinhole size. The values have been normalized by regular-RCM values (with pinhole size set to 1 Airy Unit). Gold beads (60 nm diameter) in immersion oil were imaged (see Methods), the light back-scattered by the coverslip is acting as a source of background light. Opening the pinhole in the imaging path leads to a resolution increase until it reaches a maximum plateau at 2x improvement (Figure 3h). The background rejection, which directly affects the signal-to-noise ratio of the microscope, decreases concerning the pinhole diameter. We found an optimum at a pinhole diameter of 3 Airy Units: a 2x resolution gain and a background rejection preserved at 30% as compared to regular RCM is achieved (Figure 3h).

Metrological sample imaging

We have demonstrated that the resolution of RCM can be doubled in the lateral directions and enhanced by a factor of

1.5 in the axial direction without compromising the background rejection. To validate the measurements performed on punctual objects, 3D biological samples with metrological properties have been imaged. Fossil diatom shells immersed in water (see Methods) have been considered as biological resolution targets since they have quasi-fractal structures³⁴. Figure 4a and Movies 1 and 2 (see *Extended data*)³⁵ show a 3D reconstruction of a diatom shell with both regular-RCM and the rescanned-RCM. The regular and rescanned-RCM images present notable differences: this is due to the overall 3D frequency support, which hugely differs between both modalities. The gain of resolution with rescanned-RCM is visible when using the rescanned-RCM (see in particular the insets in Figure 4a) and it shows how the small details of shells can be extracted and reconstructed in 3D. The gain in 3D (i.e. $x \rightarrow \times 2$, $y \rightarrow \times 2$, $z \rightarrow \times 1.5$) is consistent with the own measured on beads.

We have studied the effect of at-depth imaging regarding the lateral resolution improvement of rescanned-RCM versus regular-RCM. Diatom shells in agarose gel (see Methods) were imaged up to the maximum depth authorized by our microscope objective (100 μm , Figure 4b and 4c). By computing the 2D MTF at different depths starting from the coverslip ($z_0=0$) up to 100 μm , we demonstrate that the resolution

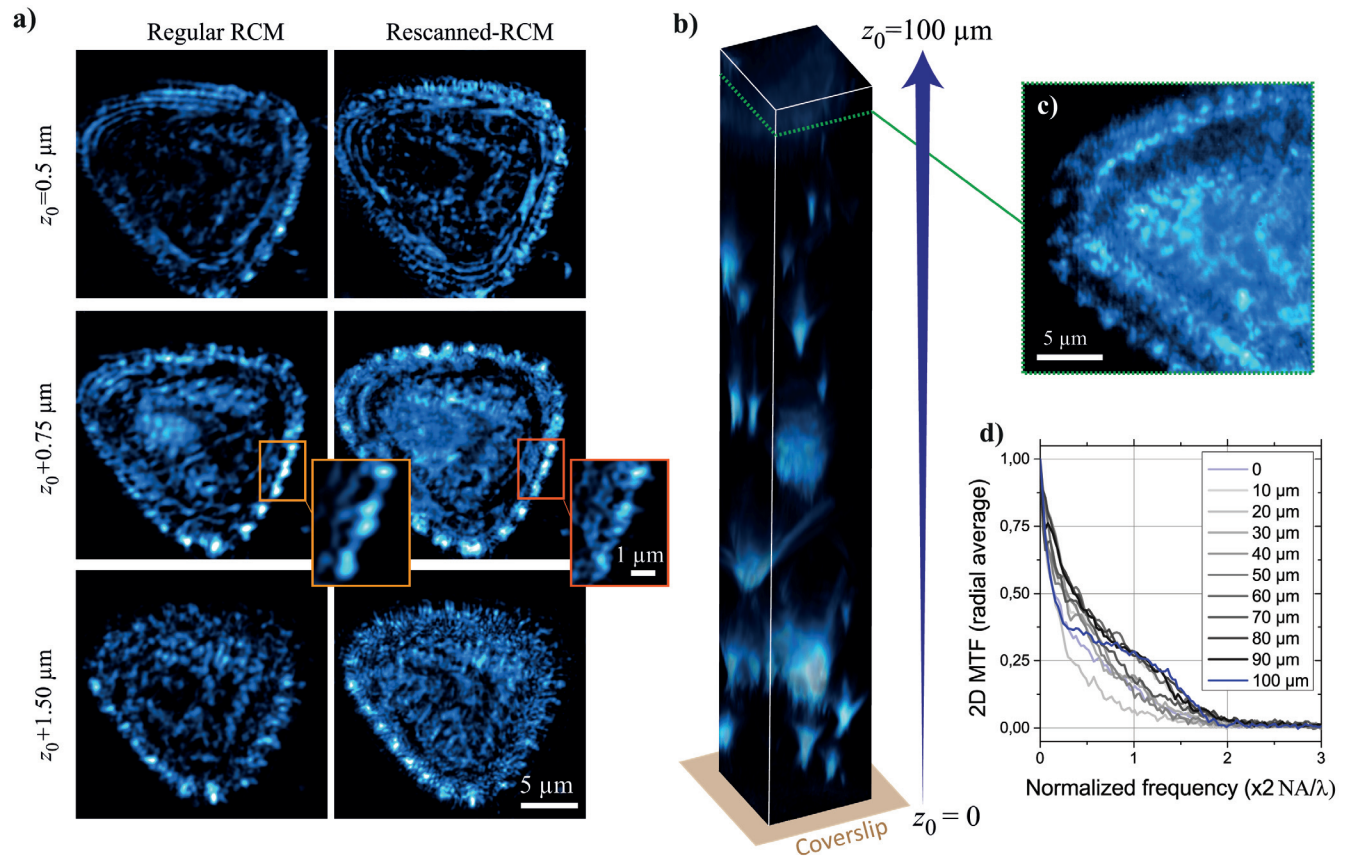


Figure 4. Diatom shells imaging in different planes. (a) From $z_0 = 0.5 \mu\text{m}$ (up) to $z_0 = 1.5 \mu\text{m}$ (down) imaged with regular reflectance confocal microscopy (RCM) (left) and rescanned RCM (right). (b) z-stack volume imaging of a diatom gel from $z_0 = 0 \mu\text{m}$ (coverslip) to $z_0 = 100 \mu\text{m}$. (c) 2D image from (b) at plane $z_0 = 95 \mu\text{m}$. (d) 2D MTFs measured on (b) at different depth from 0 to 100 μm in the sample. See Videos 1 and 2 for complete 3D visualization of the diatom shell (a).

doubling granted by rescanned-RCM is preserved at depth in scattering samples (Figure 4d).

Rescanned-RCM can also be applied in nano-material sciences to perform metrological characterization of label-free samples with unprecedented optical resolution (imaging of 90 nm diameter silver nanowires without using non-linear properties, see *Extended data: Annex 2*)³¹.

Live sample imaging

Finally, we applied rescanned-RCM to image living cells. Label-free adherent cells (mouse embryonic fibroblasts, MEF) have been observed and results are presented in Figure 5.

For fast 2D imaging (temporal resolution of 1.25 Hz), we focus on a thin part of the cell, a lamellipodium at 1 μm above the coverslip and image over time. The laser power has been reduced to limit phototoxicity (laser power of 30 μW , average power over the field-of-view of 100 W/cm^2). Such temporal resolution with limited phototoxicity allows us to discriminate and follow organelles in their native environment during minutes (no visible effect of the laser on the sample after five minutes of constant imaging).

On a large field of view (Figure 5a and 5b) the lamellipodium and membrane edges are visible in label-free, both in RCM and quantitative phase imaging³⁶. Some slowly varying fringes

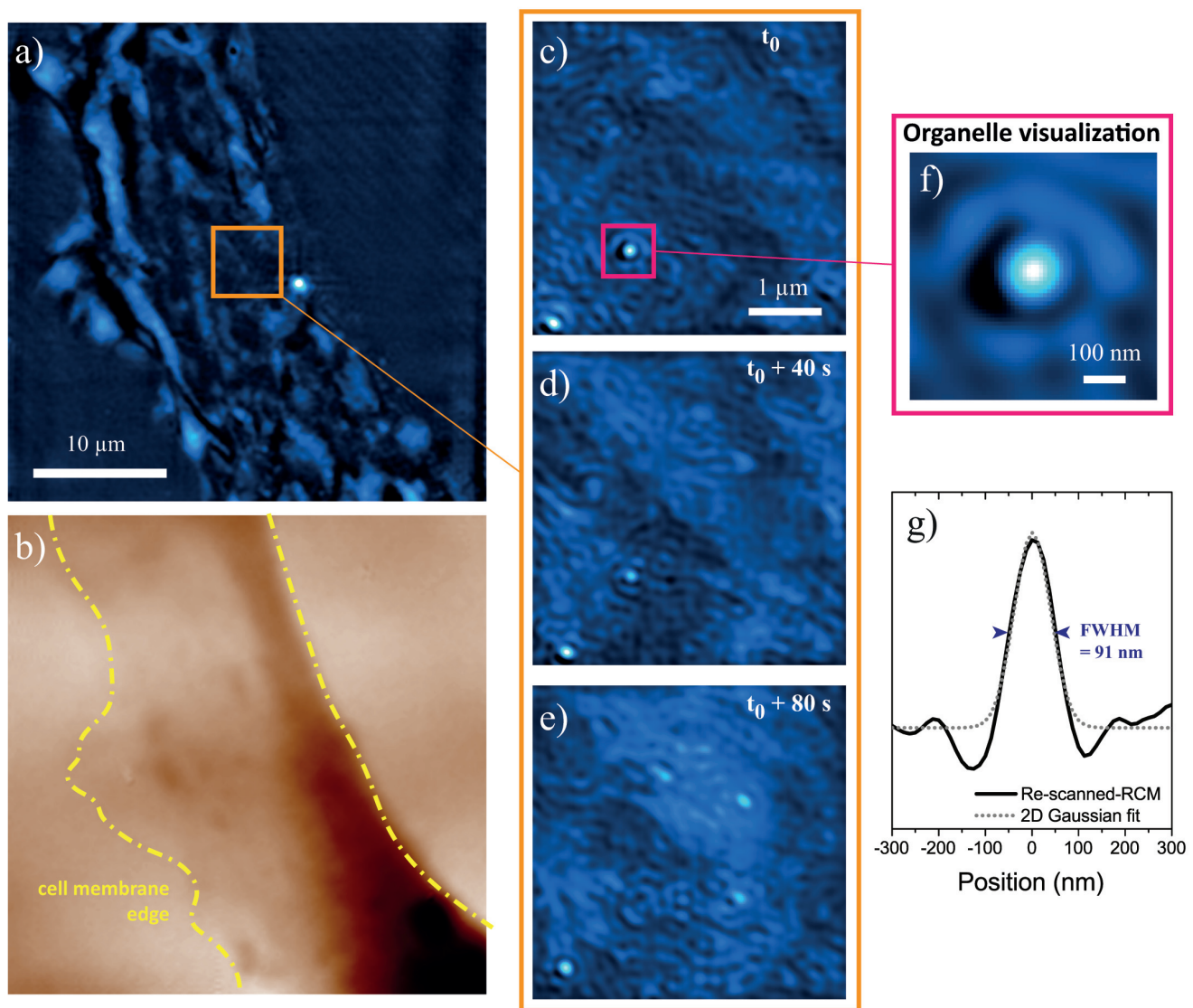


Figure 5. (a) Mouse embryonic fibroblast cell lamellipodium imaged with re-scanned reflectance confocal microscopy (RCM). (b) Same as (a) observed with quantitative phase imaging (the darker the look-up table, the longer the optical path). (c–e) Zoom on (a) at three different time points separated by 40s. (f) Zoom on a sub-structure of (b). (g) Line-out and 2D Gaussian fit of (f). All images are 2D-deconvolved. See Video 3 for the dynamic sample imaging.

are also visible in the images and are formed by the interferences between the light back-scattered from the top and the basal membrane on this thin part of the cell. Our improved resolution is key to detect and follow organelles with a very large signal-to-noise ratio (>100 , Figure 5c–e). The diameter of the detected object has been measured down to approximately 90 nm (Figure 5f and 5g) and the non-spherical shape of some organelles such as mitochondria can be studied and followed in very crowded environments without using labeling and with limited phototoxicity.

Discussion

We demonstrated that CM can reach an unprecedented 3D resolution by combining photon reassignment (originally developed for fluorescence-based CM) with label-free reflectance imaging. 3D super-resolution imaging can be achieved with an efficient background rejection and at depth imaging capabilities. Our optical photon-reassignment setup unlocks optical resolution of $(r_x, r_y, r_z)_{@z=445nm} = (86, 86, 248) \text{ nm}^3$ without requiring any computation. This is a doubled lateral resolution and $\times 1.5$ resolution improvement in the axial direction regarding regular RCM. Currently, the only far-field optical techniques that surpass our resolution are based on fluorescence photophysics (including depletion and saturation) but at the price of high-phototoxicity or sparse-labeling (single fluorescent particle imaging). Long duration live sample imaging without constraint on the sample and/or medium can only be achieved with structured illumination microscopy³⁷ and are limited to $> 100 \text{ nm}$ resolution. Our resolution improvement beyond the 100 nm resolution barrier and without requiring neither fluorescence nor computation is a new step in biological sample imaging. It unlocks studies in very crowded environments such as a living cell and at any depth within the sample, where state-of-the-art label-free techniques such as interferometric scattering (iSCAT) microscopy³⁸ reach their limits. Our approach can be applied to any samples and we have demonstrated its efficiency not only on biological samples (diatom shells and living cells) but also on nanomaterial characterization without requiring near-field or electron microscopy.

Using on-the-shelves only components, we were able to form $5 \times 5 \text{ }\mu\text{m}^2$ super-resolved images at 1.25 Hz. It has been demonstrated that the scanning speed of optical-reassignment-based methods can be tremendously increased using custom optical elements and a more challenging alignment^{26,30,39,40}. Our rescanned-RCM is a cost-effective solution for any optical microscope, the overall price of this add-on being less than 4k€ (including the laser, scanners, and camera; see Methods). This study paves the way to fully-optical fast investigations of the intimate 3D nano-structure of any samples with limited invasiveness.

Methods

Experimental setup

A 445 nm laser diode (500mW, Newgazer Technology, Shenzhen, China) is spatially filtered through a 50 μm diameter P_1 pinhole (see Figure 6) and collimated onto a 2D scanning galvo-mirror system (GVS002, Thorlabs, USA) placed in

a plane conjugated with the pupil of the microscope. The apochromatic microscope objective (UPLSAPO60XS2, 60x NA=1.3, silicon immersion, Olympus, Japan) focuses the light on the sample with a diffraction-limited d -size as shown in Figure 1. The back-scattered light is recollected by the system using the same optical path as illumination. After passing through a 50/50 non-polarized beamsplitter, the back-scattered light is filtered through a second pinhole P_2 . The size of this pinhole is directly linked to the performance of the system as discussed in results and Figure 3. In our setup, we have used a 200 μm pinhole for optimal resolution and background rejection. The light passing through the pinhole is collimated and sent on a second 2D galvo-mirror system (GVS002, Thorlabs, USA) conjugated with the pupil plane. This re-scanning mirror system redirects the collected photon onto a low-cost CMOS camera (DCC1545M, Thorlabs, USA) with a scanning amplitude of twice the amplitude of the first scanning mirror system. To compare the performance of the reflectance photon reassignment scheme and an optimal regular RCM we used an arm (Figure 6) constituted of a 90/10 non-polarized beamsplitter, a pinhole $P_3=50\mu\text{m}$ and a mono-detector (amplified photodiode). To perform z-scans, the microscope objective is moved by minimum increments of $\Delta z = 50 \text{ nm}$ (MFC-2000 Z-Axis Drive and Controller, ASI, USA). An ADC/DAC acquisition card (NIUSB-653, National Instrument USA) is used to tune the angular position of the 2D galvo mirrors (angular resolution of 15 μrad) and to digitize the amplified photodiode voltage.

Acquisition software and image processing

A homemade software written in Labview (NI LabView 2013, National Instrument USA) has been developed to drive the setup. The images don't require any further treatment to achieve super-resolution. However, for quantitative measurements, a deconvolution algorithm was applied to the raw images. The deconvolution algorithm is based on a classic Wiener filter applied considering experimental PSF and implemented in Labview. As an alternative, it is possible to use the DeconvolutionLab2 open-source software⁴¹.

Sample preparation

Gold beads. For resolution measurements, 60 nm diameter beads were used acting as punctual sources (OD 1, stabilized suspension in citrate buffer, PubChem Substance ID 329765549, Sigma Aldrich). The beads were deposited by spin-coating on a plasma cleaned cover-slip. Objective immersion oil (Nikon) was added to quasi-match the refractive index of the coverslip and minimize its back-scattered light. For studies of agglomerated but resolved objects (Figure 2b–f), 100 nm diameter gold nanobeads were used (OD 1, stabilized suspension in citrate buffer, PubChem Substance ID 329766387, Sigma Aldrich). A droplet of this solution was dried on a coverslip at room temperature for five hours to create bead clusters. As for 60 nm beads, the dried sample was immersed in immersion oil to minimize the back-scattered light from the coverslip.

Diatom shells. The diatom sample was prepared from diatomaceous earth (*La Droguerie Ecologique* - SDEB ECODIS, France) - a siliceous sedimentary rock composed of fossilized

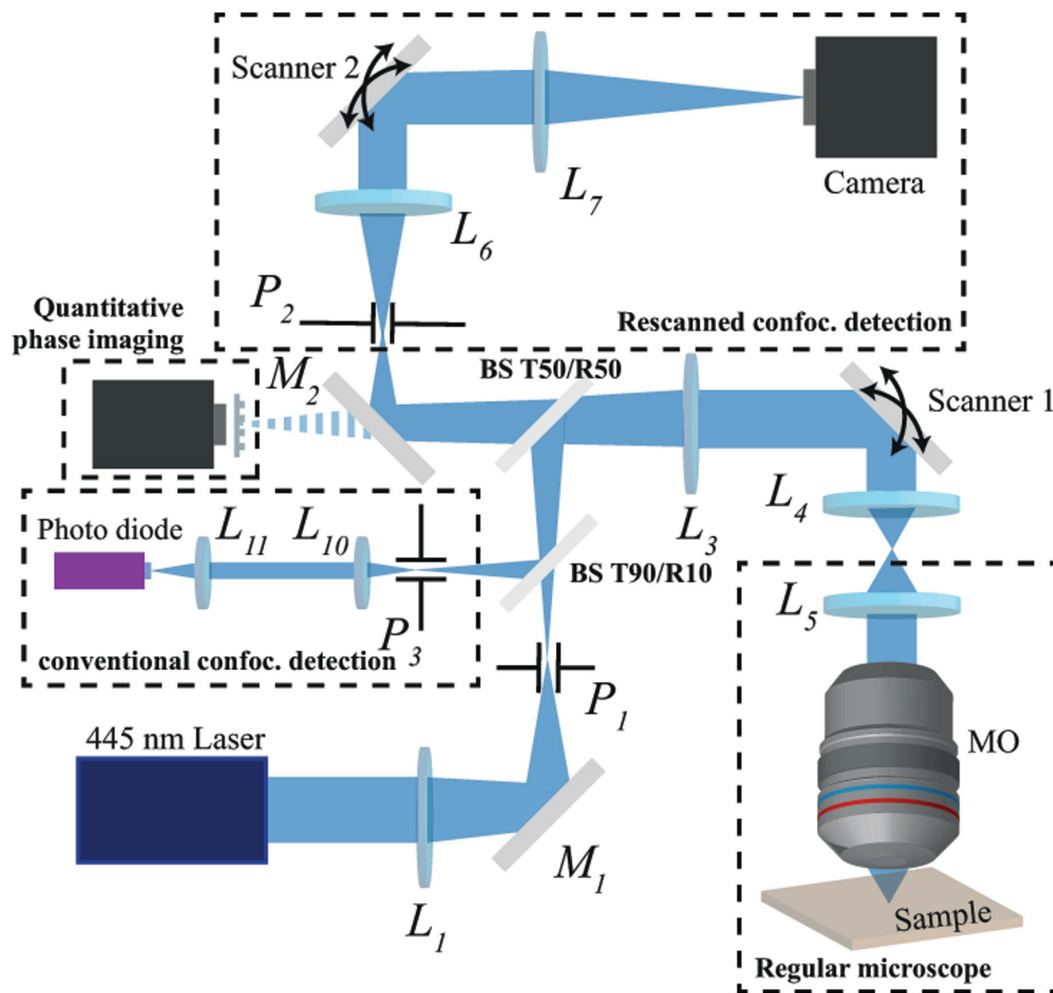


Figure 6. Complete optical setup overview. L_n are doublet lenses, M_n mirrors, P_n pinholes, TX/RX X%/Y% transmission/reflection beamsplitters, and scanners are 2D galvanometer scanners.

diatom shells- suspended in distilled water. The solution was spin-coated on a coverslip to have a uniform distribution of the diatom shells. The coverslips were immersed in distilled water to mimic biological sample imaging conditions. For thick 3D biological phantom composed of diatom shells, a 1% fossil diatom shell, 1% agarose (Low melting, Roche) solution in distilled water was prepared. The solution was then heated in the microwave 90 seconds so the agar could dissolve within the mixture. The gel was hot-deposited on a microscope coverslip. After cooling, imaging was performed.

Live cells. Wild type mouse embryonic fibroblasts (MEFs, source: courtesy of Arnaud Mourier lab). MEFs were isolated from mouse embryos of a pathogen-free C57Bl6/N mouse (Day 13.5) using classical trypsin procedure. Briefly, embryos were mechanically dispersed in presence of trypsin by repeated passage through a 1000 pipette tip and plated with MEF media (DMEM, 10% FCS, 1% nonessential amino acids, 1 mM L-glutamine, penicillin/streptomycin). Immortalization of primary MEFs was then achieved using classical viral transduction

of pMX-LargeTcDNA expressing SV40 large T antigen. Cells were grown in DMEM high glucose (4.5 g/l) with L-glutamine and sodium pyruvate supplemented with 10% FBS, and 1% penicillin-streptomycin (Corning, USA) in a humidified cell culture incubator (37°C and 5% CO₂). After several days, cells were plated at low confluency on coverslips. The rescanned-RCM imaging was performed at room temperature (24°C) in less than 30 minutes after taking the sample out of the incubator.

Data availability

Underlying data

Zenodo: Super-resolved Reflectance Confocal Microscopy data on Diatom shells and live MEF cells. <https://doi.org/10.5281/zenodo.4421019>⁴².

This project contains the following underlying data:

- Diatom images in TIF format
- Live MEF cell images in TIF format

Extended data

Zenodo: Super-resolved Reflectance Confocal Microscopy 3D reconstruction of a Diatom shell. <https://doi.org/10.5281/zenodo.4421193>³⁵.

This project contains the following extended data: back-to-back the performance in term of resolution of both standard reflectance confocal microscopy and super-resolved rescanned reflectance confocal microscopy.

- FigureDiatom-Rotation.avi (Movie 1: 3D stack angular rotation)
- FigureDiatom-Zstack.avi (Movie 2: Zstack)

Zenodo: Super-resolved Reflectance Confocal Microscopy time-lapse imaging of a living MEF cell lamellipod. <https://doi.org/10.5281/zenodo.4421233>⁴³.

This project contains the following extended data:

- FigureLamellipod.avi (time-lapse of a label-free living Mouse embryonic fibroblast cell observed

with super-resolved rescanned reflectance confocal microscopy)

Zenodo: Annex to the paper "Label-free super-resolution imaging below 90-nm using photon-reassignment". <https://doi.org/10.5281/zenodo.4421353>³¹.

This project contains the following extended data:

- Annex 1: Theory of photon reassignment super-resolution
- Annex 2: Nanomaterial imaging

Data are available under the terms of the [Creative Commons Attribution 4.0 International license](https://creativecommons.org/licenses/by/4.0/) (CC-BY 4.0).

Acknowledgements

We would like to thank L. Cognet for support, A. Mourier for the MEF cells, P. Berto for fruitful discussion and J.B. Trebbia for the silver nanowire sample.

References

1. Hell SW, Wichmann J: **Breaking the diffraction resolution limit by stimulated emission: stimulated-emission-depletion fluorescence microscopy.** *Opt Lett.* 1994; **19**(11): 780–782.
[PubMed Abstract](#) | [Publisher Full Text](#)
2. Dickson RM, Cubitt AB, Tsien RY, *et al.*: **On/off blinking and switching behaviour of single molecules of green fluorescent protein.** *Nature.* 1997; **388**(6640): 355–8.
[PubMed Abstract](#) | [Publisher Full Text](#)
3. Gustafsson MGL: **Nonlinear structured-illumination microscopy: wide-field fluorescence imaging with theoretically unlimited resolution.** *Proc Natl Acad Sci U S A.* 2005; **102**(37): 13081–13086.
[PubMed Abstract](#) | [Publisher Full Text](#) | [Free Full Text](#)
4. Betzig E, Patterson GH, Sougrat R, *et al.*: **Imaging intracellular fluorescent proteins at nanometer resolution.** *Science.* 2006; **313**(5793): 1642–1645.
[PubMed Abstract](#) | [Publisher Full Text](#)
5. Balzarotti F, Eilers Y, Gwosch KC, *et al.*: **Nanometer resolution imaging and tracking of fluorescent molecules with minimal photon fluxes.** *Science.* 2017; **355**(6325): 606–612.
[PubMed Abstract](#) | [Publisher Full Text](#)
6. Hao X, Kuang C, Gu Z, *et al.*: **From microscopy to nanoscopy via visible light.** *Light Sci Appl.* 2013; **2**: e108.
[Publisher Full Text](#)
7. Fukutake N: **A general theory of far-field optical microscopy image formation and resolution limit using double-sided Feynman diagrams.** *Sci Rep.* 2020; **10**(1): 17644.
[PubMed Abstract](#) | [Publisher Full Text](#) | [Free Full Text](#)
8. Duocastella M, Vicidomini G, Diaspro A: **Simultaneous multiplane confocal microscopy using acoustic tunable lenses.** *Opt Express.* 2014; **22**(16): 19293–19301.
[PubMed Abstract](#) | [Publisher Full Text](#)
9. Badon A, Bensussen S, Gritton HJ, *et al.*: **Video-rate large-scale imaging with Multi-Z confocal microscopy.** *Optica.* 2019; **6**(4): 389–395.
[Publisher Full Text](#)
10. Beaulieu DR, Davison IG, Kılıç K, *et al.*: **Simultaneous multiplane imaging with reverberation two-photon microscopy.** *Nat Methods.* 2020; **17**(3): 283–286.
[PubMed Abstract](#) | [Publisher Full Text](#)
11. Drexler W, Morgner U, Kärtner FX, *et al.*: **In vivo ultrahigh-resolution optical coherence tomography.** *Opt Lett.* 1999; **24**(17): 1221–1223.
[PubMed Abstract](#) | [Publisher Full Text](#)
12. Dubois A, Moneron G, Grieve K, *et al.*: **Three-dimensional cellular-level imaging using full-field optical coherence tomography.** *Phys Med Biol.* 2004; **49**(7): 1227–34.
[PubMed Abstract](#) | [Publisher Full Text](#)
13. Israelsen NM, Petersen CR, Barh A, *et al.*: **Real-time high-resolution mid-infrared optical coherence tomography.** *Light Sci Appl.* 2019; **8**: 11.
[PubMed Abstract](#) | [Publisher Full Text](#) | [Free Full Text](#)
14. Dubois A, Leveq O, Azimani H, *et al.*: **Line-field confocal optical coherence tomography for high-resolution noninvasive imaging of skin tumors.** *J Biomed Opt.* 2018; **23**(10): 1–9.
[PubMed Abstract](#) | [Publisher Full Text](#)
15. Egger MD, Petr  n M: **New Reflected-Light Microscope for Viewing Unstained Brain and Ganglion Cells.** *Science.* 1967; **157**(3786): 305–307.
[PubMed Abstract](#) | [Publisher Full Text](#)
16. Calzavara-Pinton P, Longo C, Venturini M, *et al.*: **Reflectance Confocal Microscopy for In Vivo Skin Imaging.** *Photochem Photobiol.* 2008; **84**(6): 1421–1430.
[PubMed Abstract](#) | [Publisher Full Text](#)
17. Olesen CM, Fuchs CSK, Phillipsen PA, *et al.*: **Advancement through epidermis using tape stripping technique and Reflectance Confocal Microscopy.** *Sci Rep.* 2019; **9**(1): 12217.
[PubMed Abstract](#) | [Publisher Full Text](#) | [Free Full Text](#)
18. Rajadhyaksha M, Marghoob A, Rossi A, *et al.*: **Reflectance confocal microscopy of skin in vivo: From bench to bedside.** *Lasers Surg Med.* 2017; **49**(1): 7–19.
[PubMed Abstract](#) | [Publisher Full Text](#) | [Free Full Text](#)
19. White WM, Rajadhyaksha M, Gonz  lez S, *et al.*: **Noninvasive Imaging of Human Oral Mucosa in Vivo by Confocal Reflectance Microscopy.** *Laryngoscope.* 1999; **109**(10): 1709–1717.
[PubMed Abstract](#) | [Publisher Full Text](#)
20. Issa PC, Berendschot TTJM, Staurenghi G, *et al.*: **Confocal Blue Reflectance Imaging in Type 2 Idiopathic Macular Telangiectasia.** *Invest Ophthalmol Vis Sci.* 2008; **49**(3): 1172–1177.
[PubMed Abstract](#) | [Publisher Full Text](#)
21. Xia F, Wu C, Sinefeld D, *et al.*: **In vivo label-free confocal imaging of the deep mouse brain with long-wavelength illumination.** *Biomed Opt Express.* 2018; **9**(12): 6545–6555.
[PubMed Abstract](#) | [Publisher Full Text](#) | [Free Full Text](#)
22. Schain AJ, Hill RA, Grutzendler J: **Label-free in vivo imaging of myelinated axons in health and disease with spectral confocal reflectance microscopy.** *Nat Med.* 2014; **20**(4): 443–449.
[PubMed Abstract](#) | [Publisher Full Text](#) | [Free Full Text](#)

23. Sheppard CJR: **Super-resolution in confocal imaging.** *Optik.* 1988; **80**: 53–54.
[Reference Source](#)
24. Müller CB, Enderlein J: **Image Scanning Microscopy.** *Phys Rev Lett.* 2010; **104**(19): 198101.
[PubMed Abstract](#) | [Publisher Full Text](#)
25. De Luca GMR, Breedijk RMP, Brandt RAJ, *et al.*: **Re-scan confocal microscopy: scanning twice for better resolution.** *Biomed Opt Express.* 2013; **4**(11): 2644–2656.
[PubMed Abstract](#) | [Publisher Full Text](#) | [Free Full Text](#)
26. York AG, Chandris P, Nogare DD, *et al.*: **Instant super-resolution imaging in live cells and embryos via analog image processing.** *Nat Methods.* 2013; **10**(11): 1122–6.
[PubMed Abstract](#) | [Publisher Full Text](#) | [Free Full Text](#)
27. Roider C, Ritsch-Marte M, Jesacher A: **High-resolution confocal Raman microscopy using pixel reassignment.** *Opt Lett.* 2016; **41**(16): 3825–3828.
[PubMed Abstract](#) | [Publisher Full Text](#)
28. Gregor I, Spiecker M, Petrovsky R, *et al.*: **Rapid nonlinear image scanning microscopy.** *Nat Methods.* 2017; **14**(11): 1087–1089.
[PubMed Abstract](#) | [Publisher Full Text](#)
29. Sun S, Liu S, Wang W, *et al.*: **Improving the resolution of two-photon microscopy using pixel reassignment.** *Appl Opt.* 2018; **57**(21): 6181–6187.
[PubMed Abstract](#) | [Publisher Full Text](#)
30. DuBose TB, LaRocca F, Farsiu S, *et al.*: **Super-resolution retinal imaging using optically reassigned scanning laser ophthalmoscopy.** *Nat Photonics.* 2019; **13**(4): 257–262.
[PubMed Abstract](#) | [Publisher Full Text](#) | [Free Full Text](#)
31. Aguilar A, Boyreau A, Bon P: **Annex to the paper “Label-free super-resolution imaging below 90-nm using photon-reassignment”.** *Zenodo.* 2021.
<http://www.doi.org/10.5281/zenodo.4421353>
32. Roth S, Heintzmann R: **Optical photon reassignment with increased axial resolution by structured illumination.** *Methods Appl Fluoresc.* 2016; **4**(4): 045005.
[PubMed Abstract](#) | [Publisher Full Text](#)
33. Sandison DR, Piston DW, Williams RM, *et al.*: **Quantitative comparison of background rejection, signal-to-noise ratio, and resolution in confocal and full-field laser scanning microscopes.** *Appl Opt.* 1995; **34**(19): 3576–3588.
[PubMed Abstract](#) | [Publisher Full Text](#)
34. Bismuto A, Setaro A, Maddalena P, *et al.*: **Marine diatoms as optical chemical sensors: A time-resolved study.** *Sens Actuators B Chem.* 2008; **130**(1): 396–399.
[Publisher Full Text](#)
35. Aguilar A, Boyreau A, Bon P: **Super-resolved Reflectance Confocal Microscopy 3D reconstruction of a Diatom shell.** *Zenodo.* 2021.
<http://www.doi.org/10.5281/zenodo.4421193>
36. Bon P, Maucourt G, Wattellier B, *et al.*: **Quadriwave lateral shearing interferometry for quantitative phase microscopy of living cells.** *Opt Express.* 2009; **17**(15): 13080–13094.
[PubMed Abstract](#) | [Publisher Full Text](#)
37. Li D, Shao L, Chen BC, *et al.*: **ADVANCED IMAGING. Extended-resolution structured illumination imaging of endocytic and cytoskeletal dynamics.** *Science.* 2015; **349**(6251): aab3500.
[PubMed Abstract](#) | [Publisher Full Text](#) | [Free Full Text](#)
38. Taylor RW, Mahmoodabadi RG, Rauschenberger V, *et al.*: **Interferometric scattering microscopy reveals microsecond nanoscopic protein motion on a live cell membrane.** *Nat Photonics.* 2019; **13**: 480–487.
[Publisher Full Text](#)
39. Curd A, Cleasby A, Makowska K, *et al.*: **Construction of an instant structured illumination microscope.** *Methods.* 2015; **88**: 37–47.
[PubMed Abstract](#) | [Publisher Full Text](#) | [Free Full Text](#)
40. Guo M, Chandris P, Giannini JP, *et al.*: **Single-shot super-resolution total internal reflection fluorescence microscopy.** *Nat Methods.* 2018; **15**(6): 425–28.
[PubMed Abstract](#) | [Publisher Full Text](#) | [Free Full Text](#)
41. Sage D, Donati L, Soulez F, *et al.*: **DeconvolutionLab2: An open-source software for deconvolution microscopy.** *Methods.* 2017; **115**: 28–41.
[PubMed Abstract](#) | [Publisher Full Text](#)
42. Aguilar A, Boyreau A, Bon P: **Super-resolved Reflectance Confocal Microscopy data on Diatom shells and live MEF cells [Data set].** *Zenodo.* 2021.
<http://www.doi.org/10.5281/zenodo.4421019>
43. Aguilar A, Boyreau A, Bon P: **Super-resolved Reflectance Confocal Microscopy time-lapse imaging of a living MEF cell lamellipod.** *Zenodo.* 2021.
<http://www.doi.org/10.5281/zenodo.4421233>